Published in final edited form as:

Structure. 2019 June 04; 27(6): 1022–1028.e2. doi:10.1016/j.str.2019.03.007.

Dynamics of substrate processing by PPIP5K2, a versatile catalytic machine

Yi An[1], **Henning J. Jessen**[2], **Huanchen Wang**[3], **Stephen B. Shears**[3], and **Dmitri Kireev**[1,4,*]

[1]Center for Integrative Chemical Biology and Drug Discovery, UNC Eshelman School of Pharmacy, University of North Carolina, Chapel Hill, NC 27513

[2]Institute of Organic Chemistry, University of Freiburg, 79104 Freiburg, Germany

[3]Inositol Signaling Group, Laboratory of Signal Transduction, National Institute of Environmental Health Sciences, National Institutes of Health, Research Triangle Park, NC 27709, USA

[4]Lead contact

SUMMARY

Processing of substrates by enzymes can only be fully understood through their conformational dynamics; that is particularly true for the diphosphoinositol pentakisphosphate kinase PPIP5K2, an enzyme with critical roles in cell signaling and bioenergetic homestasis. PPIP5K2 is remarkable for the reversible nature of its kinase activity, its unique ligand-stimulated ATPase activity, and the substrate travelling between two ligand-binding sites. Herein, we use molecular dynamics and data analysis techniques to rationalize these PPIP5K2 activities, thereby increasing our understanding of complex enzymatic mechanisms. In particular, we demonstrate how the enzyme's distinctive, ratchet-like mechanism harnesses the energy of random fluctuations to significantly reduce the entropy toll for intramolecular substrate transfer. We show that pre-reaction pulling forces along the reaction coordinate are predictive of the various PPIP5K2 catalytic activities. An unexpected possibility, raised by these computational studies, that 3,5-IP8 might be a substrate for dephosphorylation was experimentally interrogated and confirmed in a luciferase assay.

Graphical Abstract

*Correspondence: dmitri.kireev@unc.edu.

AUTHOR CONTRIBUTIONS

Methodology, Resources, Investigation, Analyses, Writing, & Editing: Y.A., H.J., H.W., S.S., and D.K.; Conceptualization, Writing, Review, Supervision, Project Administration: S.S. and D.K.

SUPPLEMENTAL INFORMATION

Supplemental information includes videos S1 and S2 (in MOV format), data files S1 and S2 (in XLSX format), as well as legends and notes on supplementary videos and data files (in PDF format) and can be found online.

DECLARATION OF INTERESTS

The authors declare no competing interests.

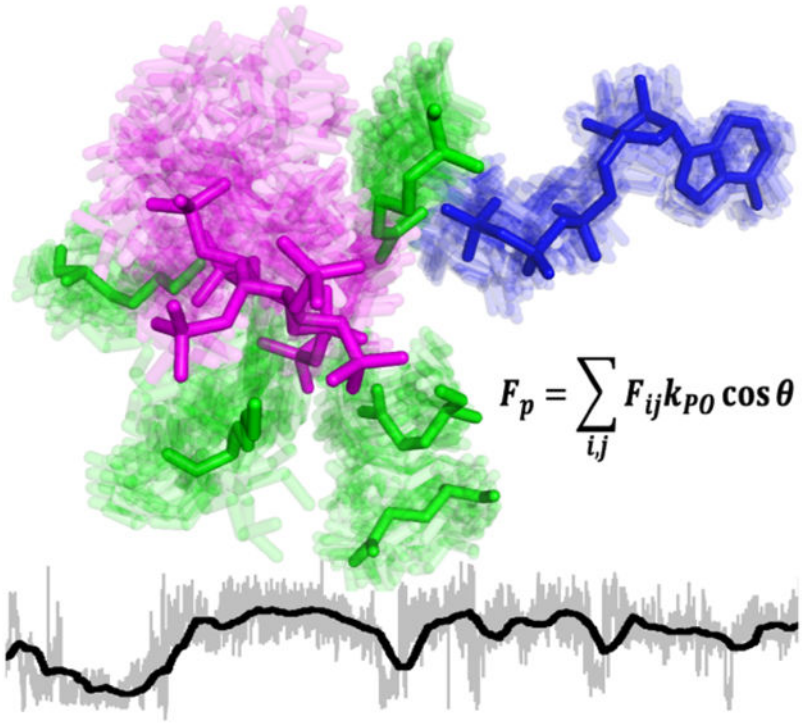

eTOC

Remarkable catalytic versatility of the pyrophosphate kinase PPIP5K2 can only be fully understood through its conformational plasticity. An et al. used molecular dynamics to study its enzymatic mechanisms. They revealed a distinctive ratchet-like mechanism of substrate transfer and showed how enzyme-substrate forces explain the enzyme's catalytic activities.

INTRODUCTION

Enzymes are extraordinary molecular machines that can increase the rate of chemical reactions in cells by many orders of magnitude. An understanding of the structural dynamics involved in enzymatic catalysis is of great benefit to synthetic biology approaches and rational drug discovery programs. While most enzymes act specifically by catalyzing a single reaction, some of them are more versatile and promote multiple reactions in response to changing cellular contexts. PPIP5K2, a diphosphoinositol pentakisphosphate kinase (Wang et al., 2012), is one such enzyme. Its biological function is of particular interest for exercising stimulus-dependent spatiotemporal control over the synthesis of inositol pyrophosphates (PP-IPs), small regulatory molecules involved in a large array of signal transduction pathways (Wilson et al., 2013). In particular, PPIP5K2 mediates cellular phosphate homestasis, since its kinase activity acts as a sensor of extracellular inorganic phosphate levels (Gu et al., 2017), dysfunctional PPIP5K2 activity in the inner ear results in hair cell loss and deafness (Yousaf et al., 2018).

Biochemically, the primary function of PPIP5K2 is 1-kinase mediated phosphorylation of 5-IP7 to form 1,5-IP8 (Shears, 2018). To a lesser extent, PPIP5K2 also phosphorylates IP6 to produce 1-IP7. Furthermore, PPIP5K2 has been shown to catalyze a reverse reaction, that is, dephosphorylation of IP8 to form 5-IP7 through transfer of a phosphate group to adenosine diphosphate (ADP) (Wang et al., 2012). Moreover, PPIP5K2 shows an incongruous substrate-stimulated ATPase activity. In addition, PPIP5K2 features a peculiar, two-step mechanism of substrate processing. The first step requires PP-IP substrate to interact with a 'capture site', a basic patch on the protein surface that imposes fewer electrostatic and structural constraints on ligand binding than does the catalytic pocket (Wang et al., 2014). In the second step, the substrate is transferred ~8 Å to the reaction site, to an orientation that is optimal to accept the γ-phosphate of ATP.

Many aspects of the mechanisms that underlie these various dynamic activities have not been elucidated using the tools of structural biology, which is limited to providing static atomic-level snapshots of various stages of a reaction processes.However, the crystal complexes that contain ligand bound to the capture site of human PPIP5K2 offer the initial atomic coordinates from which the application of classical equations of motion can yield trajectories for individual atoms in the protein and the substrate: this is the process of molecular dynamics (MD). In the current study we describe how we used MD simulations to gain considerable insight into the dynamics of the versatile molecular machine that is PPIP5K2.

For example, we depict large-scale and local conformational dynamics that move 5-IP7 substrate into the active site, in a manner that is optimal for efficient lowering of activation barriers. In particular, Principal Component Analysis (PCA) yielded considerable insight into the mechanism of the highly-unusual 'catch-and-pass' reaction mechanism, by describing a substrate trajectory in which changes in entropy are minimized. Finally, the analysis of pulling forces applied by the enzyme to the leaving γ-phosphate group of ATP along the cleavable bond unexpectedly revealed 'high-force' or 'low-force' metastable states of the catalytic pocket that are respectively more or less competent in lowering the hydrolysis activation barrier. The net lifetime of the high-force state was increased by occupation of the capture site, thereby rationalizing the enzyme's unproductive, ligand-stimulated ATPase activity.

RESULTS

Catch-and-pass substrate processing

The catalytic pocket shows a high degree of selectivity through steric constraints as well as multiple electrostatic and van der Waals interactions (Wang et al., 2012). Hence, the substrate transfer from the less constrained capture site occurs at a high entropic cost. An intriguing question is what energy currency the enzyme uses to pay the entropy toll? MD is a technique of choice to study structural details of intramolecular substrate transfer, if the time scale of the biochemical event of interest is within achievable simulation times. We have run three independent MD simulations of 1 microsecond (μs), each one including a PPIP5K2 structure, one copy of 5-IP7 in the capture site and a copy of ATP in the co-factor pocket (PDB: 4NZM; the original structure featured 5-phosphonoacetate, a close analogue of IP7,

in the capture site). In all three MD trajectories, 5-IP7 advanced at least half of the required distance, and in one simulation it fully reached the catalytic pocket. These data, which suggest that the natural transfer time is of the order of a microsecond, demonstrate the high value of MD simulations for the analysis of the enzymatic machinery. This compelling general view of the transfer process is shown in Supplementary Video 1.

Principal Component Analysis (PCA) was used to learn about the relative contributions of distinct residues and large-scale conformational rearrangements (David and Jacobs, 2014). In MD, PCA enables separation of low-frequency essential protein motions, which might correlate with biochemically relevant events, from high-frequency modes, mainly associated with random thermal fluctuations. Displacements of every residue from its initial position were used as the input to PCA (each residue was represented by two atoms, C_α and the terminal atom of the side chain; all trajectory frames were aligned using C_α atoms). All residues within 6 Å from IP7 in the capture site and from IP7 in the catalytic site (a total of 105) were involved in the analysis. Only the trajectory with the most complete path toward the catalytic site was used for this analysis. The analysis shows that, overall, motions of the residues involved are largely uncorrelated, with variance explained per principal component (PC) rapidly decaying below 1% (for 14^{th} PC) and cumulated variance of 62% explained by the first ten PCs (see full PCA data in Supplementary Table S1). Two of the three most significant PCs (PC1 and PC3) encompass large scale motions far from the capture site (Figure 1A). PC2 is more diffuse and mostly accounts for side chain motions along the substrate's pathway toward the catalytic site. None of PC1-PC3 correlates with 5-IP7 displacements. The latter only appear in PC5 along with Arg213, Gln132, Lys54, Lys103 and Glu192 (Figure 1B).

One particularly significant observation (Supplementary Video 1) is that, as 5-IP7 progresses toward the catalytic site, Glu192 moves toward the capture site to partially occupy the space left by the pyrophosphate group of 5-IP7, thus hindering the return of the substrate to its initial position. While it is intuitive that the basic side chains lining the capture site might be associated with the negatively charged 5-IP7, it is unexpected that the motions of the negatively charged Glu192 are also coordinated with substrate movement. Ultimately, the PCA data suggest that the transfer of 5-IP7 is a stochastic process involving large-scale and local thermal motions, in which the ligand trembles in all directions. There is, however, a ratchet effect that makes the random displacement of IP7 toward the catalytic site more probable than in the opposite direction, resulting in a slow but inexorable progress of IP7 towards the catalytic site. Apparently, Glu192 plays the role of a "Maxwell's demon" in this ratchet device (William Thomson). As IP7 is carried away from the capture site, the Glu192 sidechain tends to spread its fluctuations toward the vacated space and thus hinder the return of IP7 through unfavorable charge-charge interactions (Figure 1B). That is, the enzyme harnesses the energy of random fluctuations to significantly reduce the entropy toll that might have been required for a coordinated deterministic transport of the substrate. The proposed ratchet mechanism, as well as the pivotal function of Glu192 in it, is consistent with the previous mutagenesis data (Wang et al., 2014). Indeed, it has been shown that both E192G and E192Q mutations suppress the enzymatic activity of PPIP5K2, but do not affect its ATPase activity (Wang et al., 2014). These results suggest that Glu192 does not play any

role in maintaining the structural integrity of the catalytic pocket or in breaking the PO bond, but is critical for the substrate catch-and-pass mechanics.

An interesting question is how specific the proposed substrate transfer mechanism may be. A previous study has shown that, similarly to IP7, 2,5-di-O-Bn-IP4 does bind to the capture site of PPIP5K2, but then acts as an inhibitor of the "forward" phosphorylation reaction (Wang et al., 2014). Remarkably, in three MD runs (1 μs each), 2,5-di-O-Bn-IP4 did not show any significant progression toward the catalytic site (Supplementary Video 2). In two simulations the ligand remained in the capture site and in one simulation it virtually left the protein. In fact, its prolonged residence in the capture site is a likely cause of its inhibitory potency, since as long as the capture site is occupied by 2,5-di-O-Bn-IP4, the endogenous substrate would not be properly processed by the enzyme. A striking finding here is that, while the capture site is not highly selective for a particular ligand, the transfer process is. While the capture site may contribute to catalytic specificity, it is also possible that this highly unusual reaction mechanism may also participate in an endogenous inhibition mechanism by an as yet unknown, regulatory ligand.

Exposing catalytic dynamics

Ideally, *in silico* simulations of biological processes involving chemical reactions should use a quantum mechanics (QM)-based force field to accurately calculate forces in the system when chemical bonds are broken or new bonds are formed. However, QM-based simulations on biologically relevant time scales are, as yet, beyond the reach of current computing resources. Hybrid molecular mechanics (MM)/QM (Lin and Truhlar, 2007; Senn and Thiel, 2009), enable somewhat longer simulation times, but may inaccurately model large-scale protein motions because the QM portion of the system, as well as the QM/MM interface, are not optimal to model the protein dynamics (Thiel, 2009). On the other hand, many rate-determining catalytic events may lower the activation barrier prior to the actual reaction.

Therefore, even MD simulations with an MM force field may provide a wealth of information about the internal dynamics of enzymatic catalysis. Below, we (i) analyze probability density functions (PDF) for forces (F) applied to the leaving group by the protein environment along the cleavable bond (work produced by these forces contributes to lowering the activation barrier), (ii) identify structural configurations of the catalytic pocket corresponding to respectively stronger and weaker pulling forces along the cleavable bond, and (iii) estimate time scales for transitions between the high-force and low-force states. We hypothesized that this approach would expose the role of the PPIP5K2 dynamics in encoding its catalytic versatility.

Kinase reaction

PPIP5K2 phosphorylates IP7 to form 1,5-IP8 through γ-phosphate transfer from ATP. The catalytic pocket of PPIP5K2 around the leaving group is composed of 6 amino acids: His194, Arg213, Lys248, Asp308, Asp321 and Asn323. The three latter residues primarily interact with two Mg2+ ions. Hence, His194, Arg213 and Lys248, closest positively charged residues, were used in the calculations of forces potentially involved in the γ-phosphate cleavage from ATP. The x-ray structure of PPIP5K2 in complex with

phosphoaminophosphonic acid-adenylate ester (AMP-PNP), a close ATP analog, and 5-IP7 (PDB: 3T9D) was used to build the starting configuration for three independent 1 μs simulations. Despite the unexpected observation that Arg213 applies a mostly negative force (i.e., one that opposes cleavage of the γ-phosphate), the positive forces applied by Lys248 and 5-IP7 dominate throughout the simulation, in all three MD trajectories (Figure 2B and Supplementary Table S2). Most of the time, the position of the Lys248 side chain (yellow sticks in Figure 2A) yielded a force of ~2,300 pN (see PDF in Figure 2B and time charts in Figure S1). However, for ~2% of time Lys248 significantly deviated from the optimal position (red sticks in Figure 2A), which resulted in significantly lower forces of ~1,000 to 1,500 pN (Figure 2B, Supplementary Table S2). Throughout the simulation, the instantaneous net pulling force imposed upon the phosphoanhydride bond ranges from ~1,000 to ~3,000 pN. Averaging instantaneous values over 50 ns time intervals led to significantly lower force values. Ultimately, the median force over all three 1 μs simulations of the forward kinase system is 2,200 pN, that is, comparable to an experimentally determined rupture force for a covalent bond of ~2,000 pN (Grandbois et al., 1999).

ATPase activity

As is the general case with kinases (Clarke and Irvine, 2013), PPIP5K2 has a significant intrinsic ATPase activity (that is, an unproductive hydrolysis of the γ-phosphate) with vmax of 12 nmol/min/mg, ~15-fold lower than its primary, kinase activity (Wang et al., 2012; Weaver et al., 2013). However, PPIP5K2 is highly unusual in that this ATPase activity is enhanced by ligand-binding (Wang et al., 2014). In the latter study, occupation of the capture site by 2,5-di-O-Bn-IP4 was shown to have an allosteric effect on the ATP hydrolysis that has not been rationalized by the available structural and biochemical data. Here, we applied MD simulations and pulling-force analyses to investigate the ligand's role in ATPase activity. Molecular systems for three independent 1 μs MD simulations were constructed using the atomic coordinates of an x-ray structure of PPIP5K2 in complex with AMP-PNP and 2,5-di-O-Bn-IP4 (PDB code: 4NZO); the AMP-PNP was transformed into ATP. In three other simulations, 2,5-di-O-Bn-IP4 was not present in the capture site. Throughout almost the entire duration of both sets of simulations, we observed that a net positive pulling force was applied to the γ-phosphate of ATP by Lys248 (see Figures 2C-E and Supplementary Table S2). However, the PDF for simulations with and without 2,5-di-O-Bn-IP4 show significant differences. In particular, the PDF for simulation with ligand shows a rightmost peak at ~2,000 pN, and ~1,500 pN in the absence of ligand.

More importantly, the proportion of time spent by the ligand-bound system in states with instantaneous pulling forces >1,000 pN is 52% with the ligand in the capture site, compared to 19% without (Figure 2C-E and Supplementary Table S2). We investigated the latter point further by PDF analysis of the net pulling force upon ATP γ-phosphate, with or without 2,5-di-O-Bn-IP4 bound to the capture site (Figure 2C). The presence of more than one probability peak suggest distinct structural states that generate pulling forces (upon the cleavable bond) of different magnitudes. To investigate if a particular degree of pulling force is associated with a specific structural pattern, we performed a cluster analysis on cartesian atomic coordinates of aligned structures (see Supplementary Table S2 for cluster assignments of trajectory frames). We found that the major marker of a high-force structural

state is the position of Arg213, drastically shifted toward 2,5-di-O-Bn-IP4 to form a salt bridge with its 3,4-phosphate groups (Figure 2F). This shift has a dual positive effect on the net pulling force. First, it reduces the lifetime of the the orientation of Arg213 that makes a negative contribution to the net pulling force (Figure 2D,E and Supplementary Table S2). Second, when Arg213 is tethered to the ligand, away from ATP, it allows the latter to engage in a stronger interaction with Lys248, which exerts a strongly positive pulling force. These data rationalize why the simulation featuring 2,5-di-O-Bn-IP4 in the PPIP5K2 capture site spends a significantly longer time in structural configurations with a stronger pulling force (Figure 2C-E), thereby stimulating intrinsic ATPase activity. Furthermore, the pulling forces acting on the γ-phosphate observed in the system with 2,5-di-O-Bn-IP4 in the capture site are significantly weaker than those observed in the system featuring 5-IP7 in the catalytic site (Figure 2B), which may explain the lower ATPase activity compared to that required to drive the forward kinase activity.

Reverse reaction

The kinase reaction is reversible, in that PPIP5K2 catalyzes the transfer of a γ-phosphate group from 1,5-IP8 to ADP with v_{max} = 270 nmol/min/mg, that is, slightly (1.4-fold) higher than for the forward reaction (v_{max} ≈ 190 nmol/min/mg) (Wang et al., 2012). The x-ray structure of PPIP5K2 in complex with ADP and 1,5-IP8 (PDB: 4Q4C) was used to build the starting configuration for eight independent MD runs (1 μs/each). The activation barrier for hydrolysis of the 1-β-phosphate of IP8 is not known, although it is generally considered to be less than that for ATP (Hand and Honek, 2007). Indeed, the ability of PP-IPs to pyrophosphorylate proteins by a mechanism that is entirely chemical in nature is consistent with a low activation barrier for their phosphoanhydride bond cleavage (Saiardi et al., 2004). During the cumulated duration of these simulations, a positive pulling force was noted for only 19% of the time, with forces between 500 and 1700 pN observed 5% of the time. (Figure 3A,B, Supplementary Figure S2, and Supplementary Table S2). We found it difficult to distinguish between lower-force and higher-force configurations using cluster analysis (Figure 3C), although we did identify a minor reorientation of the 1-β-phosphate group of 1,5-IP8 and Lys248 (Figure 3D). As can be seen from the time charts of the pulling force (Figure 3B), positive pulling forces are not only infrequent, but also highly transient, with lifetimes on the order of nanoseconds.

3,5-IP8 is a substrate for PPIP5K2 reverse-kinase activity

We next addressed another previously intractable feature of PPIP5K2: despite its rigorous positional specificity that converts 5-IP7 to 1,5-IP8 (Wang et al., 2012), the catalytic pocket strangely lacks stereoselectivity, in that it can also accommodate 3,5-IP8, the non-natural enantiomer of 1,5-IP8 (Capolicchio et al., 2014). Based on the crystal structure of 3,5-IP8 in complex with PPIP5K2 (PDB: 4Q4C) (Capolicchio et al., 2014), it does not seem likely that 3,5-IP8 could be a substrate, because its reacting oxygen on the 3-β-phosphate group is too far (~11 Å) from the β-phosphate group of ADP. However, this prediction has not previously been tested. Three independent MD simulations (1 μs/each) were run for a system including PPIP5K2, ADP and 3,5-IP8 and respective PDF of the pulling force on 3-β-phosphate group calculated. In all three simulations, after relaxation times of up to 600 ns, systems converged to structural states in which the 3-β-phosphate of 3,5-IP8 moved closer (at ~8 Å distance) to

the oxygen β-phosphate group on ADP (Figure 3E). Typical positive pulling forces upon 3,5-IP8 (F_{max} ≈ 660 pN; 3% of time at F > 500 pN) were weaker than those upon 1,5-IP8 (F_{max} ≈ 1,700 pN; 5% of time at F > 500 pN), where F_{max} is the highest force magnitude observed during simulation. However, in the system with 3,5-IP8, positive forces were more persistent (a total of 81% of time in states with positive pulling force) (Figure 3F,G and Supplementary Table S2 for a full account of force magnitudes). This trajectory for 3,5-IP8 could not have been predicted from the static crystal complexes. Interestingly, unlike all of the reactions analyzed above, where the major contributor to the pulling force was Lys248, in the reverse reaction with 3,5-IP8, the main contribution comes from Arg213 (Figure 3F). The latter is significantly closer to the leaving phosphate group than is Lys248 (Figure 3E). In addition, we observed that Arg213 determines two structurally distinct states of the catalytic pocket: one produces a pulling force of >300 pN, but the other virtually no net force (Figure 3F).

These MD simulations raise the unexpected possibility that 3,5-IP8 might be a substrate for dephosphorylation. To interrogate this prediction a luciferase assay was used to measure the level of any ATP that might be produced (Wang et al., 2014). Control experiments were simultaneously run with 1,5-IP8 as the substrate. Both IP8 enantiomers were dephosphorylated and, in each case, the reaction rates depend hyperbolically on the concentration of substrate (Figure 3H).

DISCUSSION

In the current study, we have used MD simulations to demonstrate how conformational dynamics rationalize previously intractable aspects of a singularly remarkable molecular machine: the PPIP5K kinase domain. This enzyme's catalytic activity is reversible, it exhibits a rare ligand-stimulated ATPase activity, and the reaction process requires higher polar substrate to traverse ~8 Å between two ligand-binding sites (Wang et al., 2012, 2014). Our conclusions could not have readily been derived from structural data alone. In fact, the crystal structures used as starting points for our simulations were in general structurally far from the quasi-equilibrium system configurations.

Here, we report on an attempt to quantify the microscopic pulling forces that are required for a phosphotransfer reaction. While the force analysis proved to be a useful qualitative tool to rationalize the enzymatic activity, we also sought to assess how realistic are the quantitative levels of forces calculated in this study. Experimental assessment of interatomic forces inside a protein is not yet technically possible. However, there are rupture forces relevant to our system that have been measured by Atomic Force Microscopy (AFM): ~180 pN for hydrogen bonds to ~1,000 pN for nucleotide-nucleotide interactions to ~2,000 pN for a covalent bond (Boland and Ratner, 1995; Grandbois et al., 1999; Williams et al., 1996). In this study, highest net forces, averaged over 50 ns, ranged between ~1,000 pN in the reverse reaction system with the 1,5-IP8 substrate to ~2,700 pN in the forward reaction system (the median values over all simulations, for the above systems, were respectively −1026 pN and 2,200 pN). Thus, the forces observed in our simulations are consistent with those needed to either rupture a covalent bond (~2,000 pN) or break an ionic interaction between basic amino-acid side chains and the acidic cofactor (expected to be higher than a nucleotide-

nucleotide interaction of ~1,000 pN). Our data are also compatible with a computational study of residue-residue interactions inside the 3-Phosphogycerate kinase core, where instantaneous forces reached thousands of pN, while forces averaged over all MD trajectories were on the order of hundreds piconewtons (Palmai et al., 2014).

The information that relates to two amino acids in particular is worth highlighting. First, we have discovered that the role of Lys248 – the major driver of the net pulling force in all three endogenous systems – is more static than dynamic. That is, the Lys248 side chain does not act as an arm carrying the leaving group from one reactant to another (this would have only been possible at a high entropic cost), but is rather centered on, and thermally fluctuates around, a position enabling an optimal pulling force applied to the leaving group along the reaction coordinate. Moreover, we have shown the actions of Lys248 pulling forces are influenced by substrate binding, thereby rationalizing the hitherto perplexing ligand-stimulated ATPase. Second, we have shown how Glu192 makes a specific contribution to the ability of PPIP5K2 to harness the energy of random fluctuations to significantly reduce the entropy toll for the catch-and-pass reaction mechanism.

Finally, there is significance to experimentally verifying the prediction, drawn from the MD simulations, that 3,5-IP8 is a PPIP5K2 substrate. This supports a more general idea that the pre-reaction dynamics, and, more specifically, the analysis of pulling forces along the cleavable bond, is a valuable predictive tool. In particular, the cumulated magnitudes of the pulling-forces observed throughout our simulations are consistent with the relative values of the reaction rates for direct kinase, “reverse” kinase and ATPase activities.

STAR*METHODS

Contact for Reagent and Resource Sharing

Further information and requests for resources and reagents should be directed to and will be fulfilled by the corresponding author, Dmitri Kireev (dmitri.kireev@unc.edu).

METHOD DETAILS

Molecular dynamics—The simulations were performed using GROMACS 4.6.3 software suite with Charmm27 force field (Pronk et al., 2013; Vanommeslaeghe et al., 2010). The force field parameters of substrates (IP7, IP8) and cofactors (ADP, ATP) were obtained from SwissParam (Zoete et al., 2011). For each simulation, the particular PPIP5K2-ligand complex under study was dissolved in a 10nm × 10nm × 7nm rectangular box. The box was filled with TIP3P water. Na+ and Cl− were added using gmx genion to neutralize the system (Mark and Nilsson, 2001). Each dissolved system was first energy minimized, then equilibrated in two stages: a 500 ps run in an NVT ensemble, followed by a 2 ns run in an NPT ensemble. For each dissolved system, constant NVT simulations were performed for 1μs. In the simulation, the force was calculated every 2 fs while the coordinates were saved every 20 ps. LINCS was applied to restrain bonds, Particle Mesh Ewald (PME) was applied for long range electrostatics interactions (Essmann et al., 1995; Hess et al., 1997), modified Berendsen thermostat was used for temperature coupling (Berendsen et al., 1984), and periodic boundary condition was applied to eliminate image effects.

Principal Component Analysis—Principal Component Analysis (PCA) was performed using *prcomp* function of R software (version 3.4.2; www.r-project.org). Output was obtained in the form of PC loadings matrix (see **SI Appendix Table S1**). The input matrix of size $N_{frames} \times N_{descriptors}$, where each descriptor represents a distance from a specific atom to its position in frame 1 (i.e., $t = 0$). The atoms involved were C_α and the terminal atom of the side chain of every residue within 6 A from IP7 in the capture site and from IP7 in the catalytic site (a total of 105). Input distances were scaled to unity.

Forces along the reaction coordinate—The pulling force along the cleavable P–O bond was calculated using a custom Pipeline Pilot protocol (3dsbiovia.com). The Lennard-Jones and Coulombic terms from the Charmm27 force fiels were used to calculate the interatomic forces. PDB files exported (50,000 frames per 1 μs) from the original trajectory using the *trjconv* GROMACS tool. Interaction energy between Lys248/Arg213 and PO_4^{3-} was calculated for each frame and projected force calculated as a scalar product $F_p = \Sigma_{i,j} F_{ij} k_{PO} \cos\theta$, where F_{ij} are respective interatomic forces, k_{PO} is a unit vector in the direction of P-O bond, and $\cos\theta$ is the angle between F_{ij} and k_{PO} (see Figure 4). To avoid handling polarization effects, which might be particularly significant within the Arg213 guanidinium group, a unique positive charge of latter was centered on the central carbon atom of the group. The unique positive charge of the Lys248 amino group was placed on the ε nitrogen.

Enzyme Assays—The ADP-driven dephosphorylation of 1,5-IP8 or 3,5-IP8 by human PPIP5K2 was performed in a 96 well microplate, by incubation of 10-100nM concentrations of each substrate with the kinase domain of the protein (residues 1-366, 0.95 μg/mL) for 30 min in 20 μL buffer containing 20 mM Tris-HCl (Sigma-Aldrich), 10 mM $MgCl_2$ (Sigma-Aldrich), and 0.1 mM high purity ADP (Apollo Scientific, UK., Catalog number BIB3001HP) at pH 7.5 and T = 25 °C. Reaction s were terminated with 100 μL ice-cold, ATP-detection reagent (Invitrogen Catalog number A22066). The generated ATP was immediately recorded by Relative Luminescence using a BioTek Synergy 2 microplate reader.

QUANTIFICATION AND STATISTICAL ANALYSIS

For the ADP-driven dephosphorylation assays (Fig. 3H), values shown depict means and standard deviations from three biological replicates, all calculated using Excel.

Supplementary Material

Refer to Web version on PubMed Central for supplementary material.

ACKNOWLEDGMENTS

This work was supported by the National Institutes of Health (Grant 5R01DK101645-02), by the UNC Eshelman Institute for Innovation (Grant RX03712105), and by the Intramural Research Program of the NIH/National Institute of Environmental Health Sciences.

REFERENCES

Berendsen HJC, Postma J.P.M. van van Gunsteren WF, DiNola A, and Haak JR (1984). Molecular dynamics with coupling to an external bath. J. Chem. Phys. 81, 3684–3690.

Boland T, and Ratner BD (1995). Direct measurement of hydrogen bonding in DNA nucleotide bases by atomic force microscopy. Proc. Natl. Acad. Sci. U. S. A. 92, 5297–5301. [PubMed: 7777501]

Capolicchio S, Wang H, Thakor DT, Shears SB, and Jessen HJ. (2014). Synthesis of Densely Phosphorylated Bis-1,5-Diphospho-myo-Inositol Tetrakisphosphate and its Enantiomer by Bidirectional PAnhydride Formation. Angew. Chemie Int. Ed. 53, 9508–9511.

Clarke JH, and Irvine RF (2013). Evolutionarily conserved structural changes in phosphatidylinositol 5-phosphate 4-kinase (PI5P4K) isoforms are responsible for differences in enzyme activity and localization. Biochem. J. 454, 49–57. [PubMed: 23758345]

David CC, and Jacobs DJ (2014). Principal Component Analysis: A Method for Determining the Essential Dynamics of Proteins. (Humana Press, Totowa, NJ), pp. 193–226.

Essmann U, Perera L, Berkowitz M, Darden T, Lee H, and Pedersen L (1995). A smooth particle mesh Ewald method. J Chem Phys 103, 8577–8593.

Grandbois M, Beyer M, Rief M, Clausen-Schaumann H, and Gaub HE (1999). How strong is a covalent bond? Science 283, 1727–1730. [PubMed: 10073936]

Gu C, Nguyen H-N, Hofer A, Jessen HJ, Dai X, Wang H, and Shears SB (2017). The Significance of the Bifunctional Kinase/Phosphatase Activities of Diphosphoinositol Pentakisphosphate Kinases (PPIP5Ks) for Coupling Inositol Pyrophosphate Cell Signaling to Cellular Phosphate Homeostasis. J. Biol. Chem. 292, 4544–4555. [PubMed: 28126903]

Hand CE, and Honek JF (2007). Phosphate transfer from inositol pyrophosphates InsP5PP and InsP4(PP)2: A semi-empirical investigation. Bioorg. Med. Chem. Lett. 17, 183–188. [PubMed: 17045478]

Hess B, Bekker H, Berendsen HJC, and Fraaije JGEM (1997). LINCS: a linear constraint solver for molecular simulations. J. Comput. Chem. 18, 1463–1472.

Lin H, and Truhlar DG (2007). QM/MM: what have we learned, where are we, and where do we go from here? Theor. Chem. Acc. 117, 185.

Mark P, and Nilsson L (2001). Structure and Dynamics of the TIP3P, SPC, and SPC/E Water Models at 298 K. J. Phys. Chem. A 105, 9954–9960.

Palmai Z, Seifert C, Gräter F, and Balog E (2014). An Allosteric Signaling Pathway of Human 3-Phosphoglycerate Kinase from Force Distribution Analysis. PLoS Comput. Biol. 10, e1003444. [PubMed: 24465199]

Pronk S, Páll S, Schulz R, Larsson P, Bjelkmar P, Apostolov R, Shirts MR, Smith JC, Kasson PM, and van der Spoel D (2013). GROMACS 4.5: a high-throughput and highly parallel open source molecular simulation toolkit. Bioinformatics 29, 845–854. [PubMed: 23407358]

Saiardi A, Bhandari R, Resnick AC, Snowman AM, and Snyder SH (2004). Phosphorylation of proteins by inositol pyrophosphates. Science 306, 2101–2105. [PubMed: 15604408]

Senn HM, and Thiel W (2009). QM/MM Methods for Biomolecular Systems. Angew. Chemie Int. Ed. 48, 1198–1229.

Shears SB (2018). Intimate connections: Inositol pyrophosphates at the interface of metabolic regulation and cell signaling. J. Cell. Physiol. 233, 1897–1912. [PubMed: 28542902]

Thiel W (2009). QM/MM Methodology: Fundamentals, Scope, and Limitations. In Multiscale Simulation Methods in Molecular Sciences, Grotendorst DMJ, Attig N, Blügel S, ed. (Institute for Advanced Simulation,), pp. 203–214.

Thomson W (1879). The Sorting Demon Of Maxwell. From Pop. Lect. Addresses 144–148.

Vanommeslaeghe K, Hatcher E, Acharya C, Kundu S, Zhong S, Shim J, Darian E, Guvench O, Lopes P, Vorobyov I, et al. (2010). CHARMM general force field: A force field for drug-like molecules compatible with the CHARMM all-atom additive biological force fields. J. Comput. Chem. 31, 671–690. [PubMed: 19575467]

Wang H, Falck JR, Hall TMT, and Shears SB (2012). Structural basis for an inositol pyrophosphate kinase surmounting phosphate crowding. Nat Chem Biol 8, 111–116.

Wang H, Godage HYY, Riley AMM, Weaver JDD, Shears SBB, and Potter BVLVL (2014). Synthetic Inositol phosphate analogs reveal that PPIP5K2 has a surface-mounted substrate capture site that is a target for drug discovery. Chem. Biol. 21, 689–699. [PubMed: 24768307]

Weaver JD, Wang H, and Shears SB (2013). The kinetic properties of a human PPIP5K reveal that its kinase activities are protected against the consequences of a deteriorating cellular bioenergetic environment. Biosci. Rep. 33.

Williams JM, Han T, and Beebe TP (1996). Determination of Single-Bond Forces from Contact Force Variances in Atomic Force Microscopy. Langmuir 12, 1291–1295.

Wilson MSC, Livermore TM, and Saiardi A (2013). Inositol pyrophosphates: between signalling and metabolism. Biochem. J. 452, 369–379. [PubMed: 23725456]

Yousaf R, Gu C, Ahmed ZM, Khan SN, Friedman TB, Riazuddin S, Shears SB, and Riazuddin S (2018). Mutations in Diphosphoinositol-Pentakisphosphate Kinase PPIP5K2 are associated with hearing loss in human and mouse. PLOS Genet. 14, e1007297. [PubMed: 29590114]

Zoete V, Cuendet MA, Grosdidier A, and Michielin O (2011). SwissParam: A fast force field generation tool for small organic molecules. J. Comput. Chem. 32, 2359–2368. [PubMed: 21541964]

HIGHLIGHTS

- Molecular dynamics was used to rationalize the catalytic versatility of PPIP5K2.
- A distinctive ratchet mechanism is involved in intramolecular substrate transfer.
- Enzyme-substrate forces are predictive of the various PPIP5K2 catalytic activities.
- A new substrate was computationally predicted and experimentally confirmed.

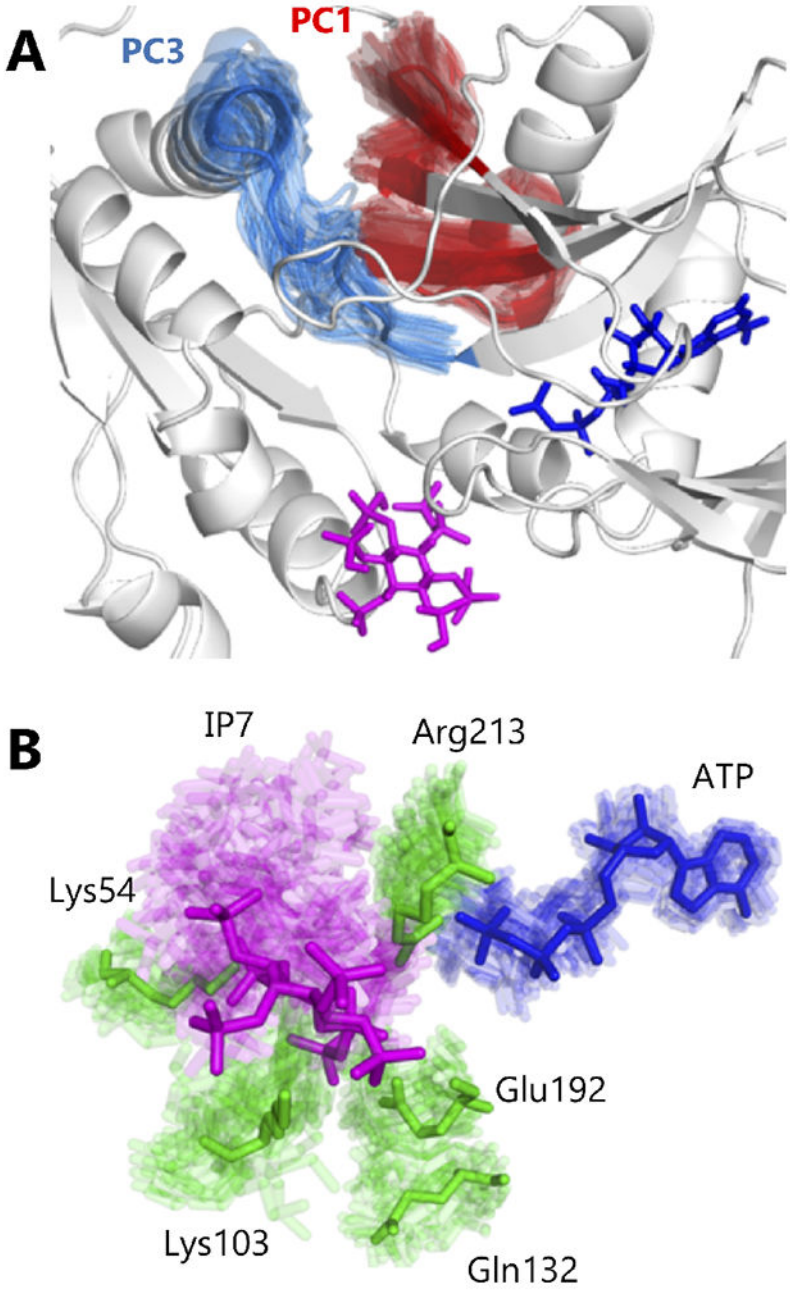

Figure 1.

(A) Sampled large scale motions encompassed by PC1 (res. 251-259, 298-307)(red transparent cartoons) and PC3 (res. 327-335)(blue transparent cartoons).

(B) Trace of the IP7 (magenta) progression toward the catalytic site and residues (green) whose displacements correlate with those of IP7.

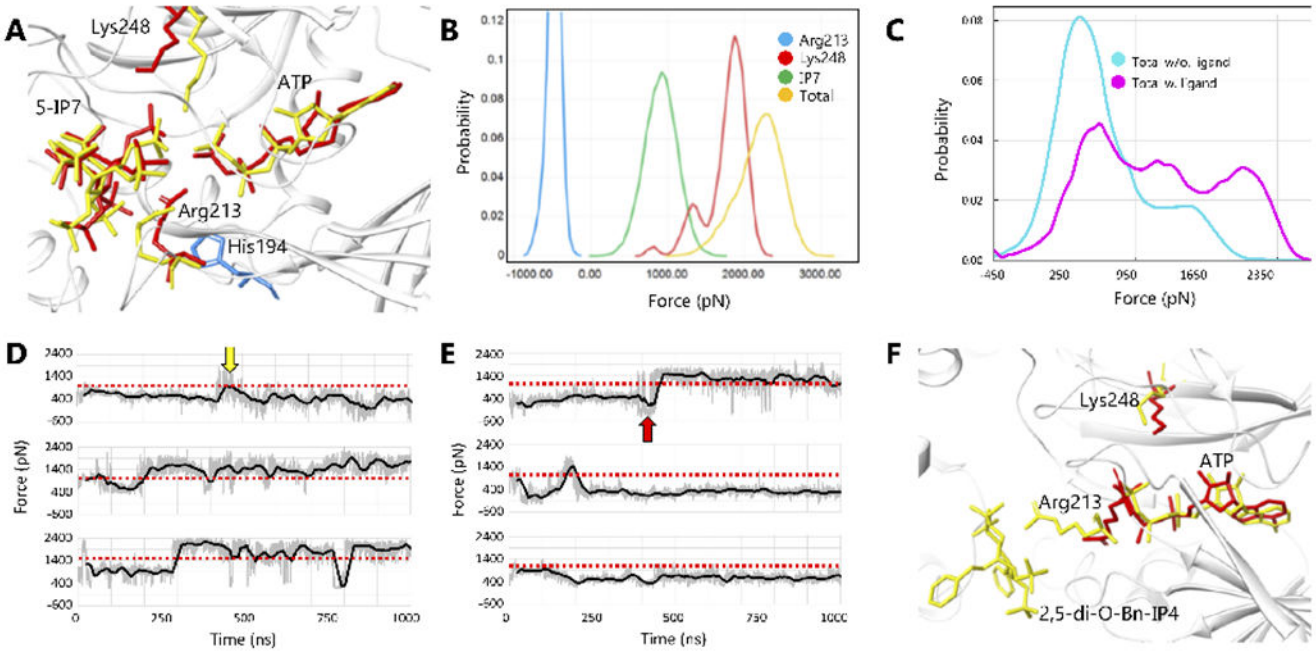

Figure 2.

(A) Structure of the active site containing 5-IP7 substrate; yellow and red sticks depict highest (F=3322 pN at t=541 ns) and lowest (F=874 pN at t=168 ns) instantaneous force conformations, respectively;

(B) PDF of the net pulling force upon ATP γ-phosphate and its components in the forward reaction system with 5-IP7 as substrate;

(C) PDF of the net pulling force upon ATP γ-phosphate in the ATPase reaction system with (magenta) or without (cyan) 2,5-di-O-Bn-IP4 in the capture site;

(D) and (E) time courses of the net pulling force in the ATPase reaction system, with and without 2,5-di-O-Bn-IP4 respectively; instantaneous MD forces are shown in light gray; the moving average curve, over 50 ns, is shown as a solid black line; the red dotted line is an arbitrary separator (at 1,000 pN) between high and low forces in the context of the ATPase reaction. The yellow and red arrows indicate at which point of the respective simulations the yellow and red conformations shown in Figure 2F occurred.

(F) A typical high-force (F= 1407 pN at t=460.90 ns)(yellow sticks) and a low-force (F= −667 pN at t=410.32 ns)(red sticks) states of the catalytic pocket in the ATPase reaction system, respectively with and without 2,5-di-O-Bn-IP4 in the capture site.

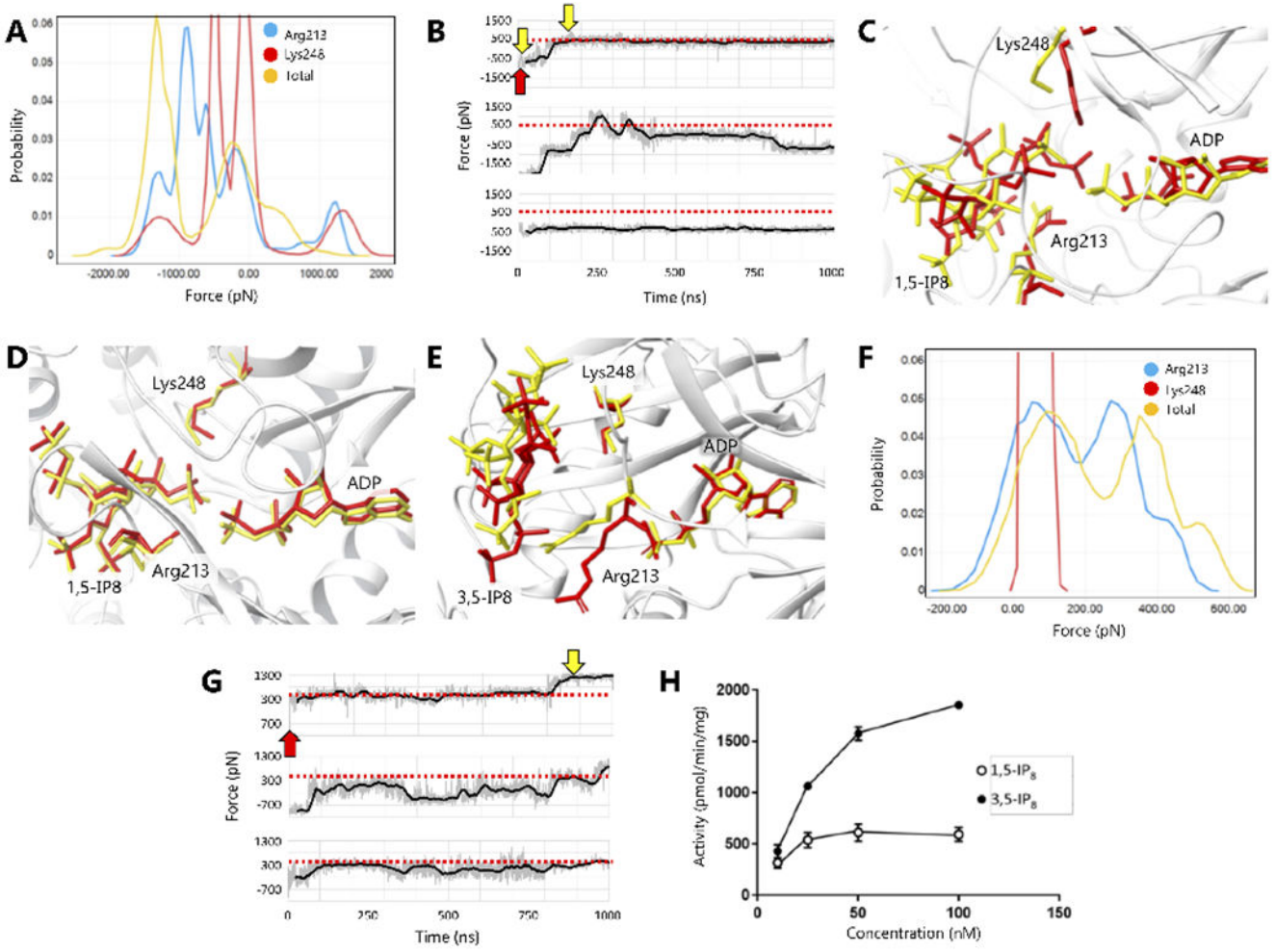

Figure 3.

(A) PDF of the net pulling force upon 1-β-phosphate in 1,5-IP8 and its components in the reverse reaction system;

(B) and (G) time courses of the net pulling force in the reverse reaction system, with 1,5-IP8 and 3,5-IP8 substrates respectively; instantaneous MD forces are shown in light gray; the moving average curve, over 50 ns, is shown as a solid black line; the red dotted line is an arbitrary separator (at 500 pN) between high and low forces in the context of the reverse reaction; The yellow and red arrows indicate at which point of the respective simulations the yellow and red conformations shown in Figures 3C-E occurred; Three representative trajectories, out of 8, are shown in Fig. 3B (see Suppl. Fig. S2 for the remaining five trajectories).

(C) Structure of the active site containing 1,5-IP8 substrate; yellow and red sticks depict positive (F= 86 pN at t=8.80 ns) and highly negative (F=−919 pN at t=0.24 ns) instantaneous force conformations, respectively, showing significant structural differences;

(D) Structure of the active site containing 1,5-IP8 substrate; yellow and red sticks depict transient, structurally similar high (F= 967 pN at t=165.22 ns) and low (F=−919 pN at

t=0.24 ns) instantaneous force conformations, respectively, differing only in orientation of of the 1-β-phosphate group;

(E) Structure of the active site containing 3,5-IP8 substrate; yellow and red sticks depict transient, structurally similar high (F= 1117 pN at t=875 ns) and low (F= −1071 pN at t=1.20 ns) instantaneous force conformations, respectively;

(F) PDF of the net pulling force upon 3-β-phosphate in 3,5-IP8 and its components in the reverse reaction system with 3,5-IP8 as potential substrate;

(H) rate of PPIP5K2-mediated dephosphorylation of either 1,5-IP8 or 3,5-IP8 as a function of their concentration; assays were performed with 100 μM ADP at 25°.

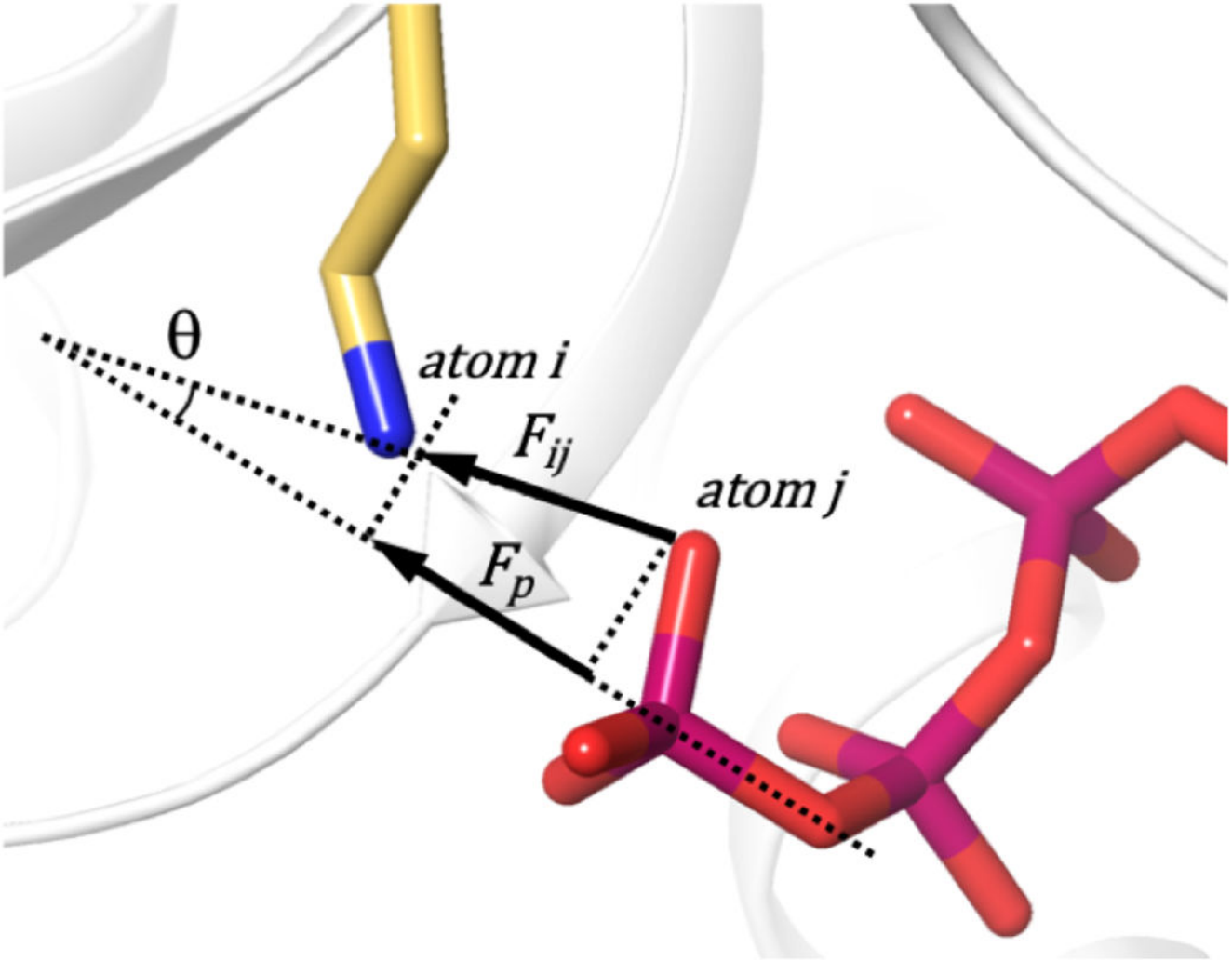

Figure 4.
Calculation of the force projection F_p along the reaction coordinate for a pair of atoms *i* and *j*.

KEY RESSOURCES TABLE

RESOURCE	SOURCE	IDENTIFIER
Commercial assays		
Luciferase assay	Invitrogen	Catalog# A22066
Chemicals, peptides, and proteins		
PPIP5K2 kinase domain	Wang et al., 2012	N/A
1,5-IP8	Capolicchio et al., 2014	N/A
3,5-IP8	Capolicchio et al., 2014	N/A
ADP	Apollo Scientific	Catalog# BIB3001 HP
Tris-HCl	Sigma-Aldrich	Catalog# 10812846001
$MgCl_2$	Sigma-Aldrich	Catalog# M8266
Software		
GROMACS 4.6.3	GROMACS project	www.gromacs.org
Maestro molecular modeling suite 2017-1	Schrödinger	www.schrodinger.com
R Statistical computing and graphics	R project	www.r-project.org
Pipeline Pilot (data processing software)	BIOVIA	www.3ds.com